

Color Enhancement for Low Blue Light Display Modes

Yu-Heng Su
113062539

CS, National Tsing Hua University

Li-Ting Huang
113065503

ISA, National Tsing Hua University

Nien-Heng Yu
113061516

EE, National Tsing Hua University

I. INTRODUCTION

To reduce eye strain and improve sleep quality, many users adopt low blue light display modes such as f.lux or Night Shift during nighttime usage. These modes work by suppressing short-wavelength blue light, which has been shown to affect circadian rhythms and melatonin secretion. While this practice provides physiological benefits, it comes at the cost of significant visual drawbacks.

One of the most evident issues is color distortion. As shown in both textual interfaces and natural images, low blue light modes can alter the appearance of colors, making them less distinguishable or merging distinct hues. This negatively impacts visual tasks that rely on accurate color representation, such as programming (due to reduced syntax highlighting clarity) and content creation.

Recent research (Shih et al., ACM TOG 2016) [10] highlights that this problem stems from the fact that current blue light filtering strategies indiscriminately suppress a broad spectral range. However, the intrinsically photosensitive retinal ganglion cells (ipRGCs), which are primarily responsible for non-visual effects of light, are sensitive to a narrow band near 482nm — a range distinct from the cones responsible for color vision. This key insight implies that it is possible to reduce ipRGC stimulation while preserving overall color appearance.

In this work, we aim to develop a **color compensation method** tailored for low blue light mode. Our goal is to restore color discriminability and perceptual quality without undermining the blue light suppression effect. By preserving both user comfort and color fidelity, we seek to enhance the usability of low blue light displays across a variety of visual applications.

II. METHOD

To enhance color fidelity and vividness, simply operating within the sRGB space is insufficient. The Euclidean distance between two RGB values does not accurately reflect perceptual differences as experienced by the human visual system. Therefore, various color appearance models have been developed to better mimic human color perception. Notable examples include the RLAB, Hunt, and CIECAM02 models, which aim to more closely align with the principles described by the von Kries hypothesis.

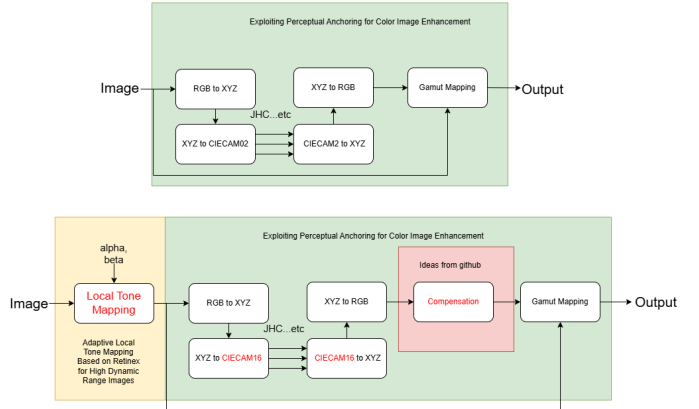


Fig. 1: Methods overview

We build upon the original pipeline introduced in [8], and further improve it by integrating preprocessing and post-processing techniques inspired by other research papers and public GitHub repositories. These enhancements contribute significantly to the overall performance and quality of the final results. An overview of the proposed method, including key components in preprocessing, core processing, and post-processing, is illustrated in Fig. 1.

A. Pre-process

We adapt the tone mapping as a pre-process to enhance the stability. The local adaptation equation can be written as

$$L_l(x, y) = \log L_g(x, y) - \log H_g(x, y), \quad (1)$$

where $L_l(x, y)$ denotes the local adaptation output, and $H_g(x, y)$ is the output of the guided filter applied to $L_g(x, y)$.

After that, to prevent the flat-looking appearance caused by the filter and improve the performance of our method, we introduce two important factors.

$$\alpha(x, y) = 1 + \eta \frac{L_g(x, y)}{L_{g,\max}}, \quad (2)$$

where η denotes the contrast control parameter, and $L_{g,\max}$ is the maximum luminance value of the original image.

The second, the adaptive nonlinearity offset, which varies in accordance with the scene contents, is defined as:

$$\beta = \lambda \bar{L}_g, \quad (3)$$

where λ is the nonlinearity control parameter, and \bar{L}_g is the log-average luminance of the original image.



Fig. 2: With / Without pre-process.

By integrating these factors into equation is established as follows:

$$L_{\text{out}}(x, y) = \alpha(x, y) (\log L_g(x, y) - \log H_g(x, y)) + \beta, \quad (4)$$

where $L_{\text{out}}(x, y)$ is the final output for pre-process.

The impact of this pre-processing step can be visually observed in Fig. 2, which compares images with and without applying our local adaptation strategy.

B. Core function

With the pre-process ready, move on to the core function for the whole methods, which performs perceptual color adaptation based on the **CIECAM16** model.

- 1) The input RGB image is normalized and flattened to extract unique colors, reducing redundant computation. These colors are converted to the CIE 1931 XYZ space using device-specific colorimetric transformations.
- 2) The white points corresponding to daylight (D65) and the target illumination temperature (e.g., 2700K) are calculated. The model then transforms colors from the source to target lighting condition via forward and

inverse CIECAM16 adaptations, leveraging parallel processing for efficiency.

The perceptual fidelity of the result is quantified by computing the product of lightness and chroma ($J \cdot C$) for each pixel. Finally, the image is reconstructed in RGB space and clipped to ensure display validity. This function provides a robust and efficient simulation of color appearance changes under varying ambient lighting conditions.

C. Post-Process

To ensure perceptual validity and maintain image detail, a post-processing step is applied to handle out-of-gamut values (i.e., RGB components falling outside the $[0, 1]$ range). After performing CIECAM-based color adaptation, some pixels may lie beyond the representable color gamut. To correct this, we apply a linear interpolation between the original RGB values and their clipped counterparts using the pixel-wise JC value (product of lightness J and chroma C) as the blending weight. As shown in Eq. 5,

$$\begin{bmatrix} R_e \\ G_e \\ B_e \end{bmatrix} = (1 - JC) \begin{bmatrix} R_c \\ G_c \\ B_c \end{bmatrix} + JC \begin{bmatrix} R_i \\ G_i \\ B_i \end{bmatrix}, \quad (5)$$

where $[R_c, G_c, B_c]$ are the clipped values and $[R_i, G_i, B_i]$ are the original adapted values. This weighting scheme favors the original values in bright and saturated regions, preserving vivid details while avoiding color distortion.

We also observe that further increasing the original pixel intensity $[R_c, G_c, B_c]$ prior to gamut mapping can sometimes produce more visually satisfactory results. When an additional compensation step is applied (by re-adjusting the image using the same RGB scaling factors and averaging the outcome with the initial compensation), the final image often exhibits enhanced brightness and contrast. This dual compensation approach is particularly effective in underexposed or color-biased regions, contributing to improved overall visual fidelity.

The visual impact of the proposed post-processing strategy is shown in Fig. 3, which compares the results with and without post-processing.

III. EXPERIMENT

A. Experiment Setting

To reconstruct the spectral characteristics of display devices, a spectral mapping approach was formulated based on experimental measurements. The objective is to predict the spectral power distribution (SPD) from RGB input values under varying correlated color temperatures, thereby enabling the estimation of metrics such as Equivalent Melanopic Lux (EML).

1) Measurement Setup

Spectral data were acquired using a spectrometer (SpectraSmart DS1200) [11] across the following measurement types:

- **Monochrome spectrum:** The display showed varying green values, and the resulting SPDs were measured.



Fig. 3: With/Without post process.

- **Mixed RGB spectrum:** The display showed hybrid RGB values, and the resulting SPDs were measured.
- **Color temperature variation spectrum:** The display showed varying RGB values under 2700K–6500K (500K steps), and the resulting SPDs were measured. One of the three tested displays was used for spectral mapping.

2) RGB to SPD Mapping with Gamma Correction

Measured data revealed that RGB values and SPDs exhibit an approximately linear relationship after gamma correction is applied to the spectral data [12]. Based on this, the SPD for a given RGB input can be reconstructed using the following expressions:

$$\begin{aligned}\text{spectrum}_R &= \left[\frac{R}{255} \cdot \left(S_R^{1/\gamma} \right) \right]^\gamma \\ \text{spectrum}_G &= \left[\frac{G}{255} \cdot \left(S_G^{1/\gamma} \right) \right]^\gamma \\ \text{spectrum}_B &= \left[\frac{B}{255} \cdot \left(S_B^{1/\gamma} \right) \right]^\gamma\end{aligned}$$

$$\text{spectrum}_{RGB} = \text{spectrum}_R + \text{spectrum}_G + \text{spectrum}_B$$

Here, S_R , S_G , and S_B represent the measured SPDs of the red, green, and blue channels of full intensity, respectively. The optimal gamma value was empirically determined to be $\gamma = 2.24$ for our display, minimizing the mean relative error between the reconstructed and measured spectra.

3) Model Validation and Applications

To evaluate performance, the mapping approach was tested using unseen hybrid RGB inputs. The reconstructed SPDs closely matched the measured spectra in both energy distribution and peak wavelength. As shown in Fig. 4, the predicted spectrum for $RGB = (85, 255, 128)$ shows strong agreement with the measured result. The red dashed curve represents the

spectrum generated from the RGB input, while the black solid curve shows the spectrum captured by the spectrometer.

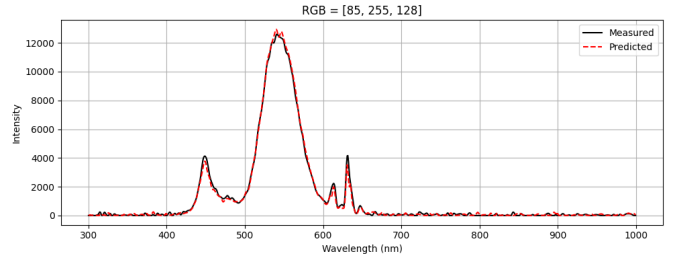


Fig. 4: Comparison of measured and predicted SPD for $RGB = (85, 255, 128)$.

The resulting RGB to SPD mapping enables accurate prediction of blue light exposure metrics, including total blue energy and Equivalent Melanopic Lux (EML). These metrics are essential for estimating the amount of blue light received by the human visual and circadian systems under low-blue-light display conditions.

B. Evaluation Metrics

Evaluating visual quality from a human perspective is inherently challenging. Although SSIM is widely used for image quality assessment, it is unsuitable for our task, which places particular emphasis on color fidelity. As Nilsson and Akenine-Möller pointed out [4], many distinct colors can share the same luminance, and any mapping from RGB to grayscale is fundamentally many-to-one. As a result, converting RGB images to grayscale can yield misleading SSIM scores, as can any metric that relies on such a dimensionality reduction. Therefore, SSIM is inappropriate for evaluating color images, especially in applications where accurate color differences are crucial, as in our work.

To this end, We adopted four common used metrics for the evaluation:

- 1) CIEDE2000 color difference (ΔE_{2000})
- 2) Chromaticity difference ($\Delta u'v'$)
- 3) Distance from Planckian locus (D_{uv})
- 4) Equivalent Melanopic Lux (EML)

CIEDE2000 color difference (ΔE_{2000}). This metric quantifies perceptual color differences by incorporating corrections for lightness (L^*), chroma (C^*), hue (H^*), and interactive effects between them. Compared to earlier ΔE formulas, CIEDE2000 provides significantly improved perceptual uniformity, and is widely regarded as the most accurate color difference metric for modeling human visual perception [5], [8], where similar evaluation needs were addressed.

Chromaticity difference ($\Delta u'v'$). It is a color difference metric defined in the CIE 1976 (u' , v') uniform chromaticity scale diagram. It is calculated as the Euclidean distance between two chromaticities:

$$\Delta u'v' = \sqrt{(u'_2 - u'_1)^2 + (v'_2 - v'_1)^2} \quad (6)$$

This metric reflects perceptual color differences more accurately than (x, y) coordinates. A $\Delta u'v'$ value less than 0.02 is generally regarded as below the just-noticeable difference (JND) threshold for human vision, meaning the difference is typically imperceptible to the average observer [6], [7].

Distance from Planckian locus (D_{uv}). D_{uv} is defined as the orthogonal distance from the chromaticity coordinate of a test light source to the nearest point on the Planckian (blackbody) locus [9], with positive values indicating positions above the curve (greenish hue) and negative values below it (pinkish hue).

Equivalent Melanopic Lux (EML). While traditional metrics such as ΔE_{2000} or $\Delta u'v'$ focus on perceived chromatic differences, they do not account for the non-visual physiological effects of light. In our work, color compensation under low blue light conditions must not only preserve visual appearance, but also respect the original intention of reducing short-wavelength (blue) light exposure. Excessive restoration of blue components may counteract the intended circadian benefits of low-blue-light modes.

To address this, we adopt Equivalent Melanopic Lux (EML) as a non-visual performance metric. Unlike conventional photopic lux, which reflects the spectral sensitivity of cones responsible for visual perception, melanopic lux captures the biological effects of light mediated by intrinsically photosensitive retinal ganglion cells (ipRGCs), which regulate circadian rhythms and melatonin production. Therefore, EML provides a more appropriate measure of the biological impact of light exposure.

We follow the evaluation method of Xu et al. [1], and compute EML based on the definition in CIE S026/E:2018 [2], [3], by integrating the product of the photopic spectral irradiance $E_{e,\lambda}(\lambda)$ and the normalized melanopic action spectrum $N_\alpha(\lambda)$, as shown in Eq. (7).

$$\text{EML} = 72983.25 \int_{380}^{780} E_{e,\lambda}(\lambda) N_\alpha(\lambda) d\lambda \quad (7)$$

C. Quantitative Results

To ensure generalization, we collected a diverse set of images covering multiple categories and scenes, including 10 camera-captured images and 10 screenshots. We evaluate our method using standard perceptual and photobiological metrics, including ΔE , $\Delta u'v'$, D_{uv} , and EML. The quantitative results are summarized in Table I and II.

Method	ΔE	$\Delta u'v'$	D_{uv}	EML
Original (6500K)	0	0	-0.0027	208.6081
2700K lighting	17.5914	0.0893	-0.0048	54.6602
Our method	14.2845	0.0481	-0.0023	76.068

TABLE I: Average perceptual and biological metrics on camera-captured images.

Compared with the 2700K mode, our proposed compensation method reduces perceptual color errors by 18.8% in ΔE and 46.14% in $\Delta u'v'$ on camera-captured images, and by

Method	ΔE	$\Delta u'v'$	D_{uv}	EML
Original (6500K)	0	0	-0.0021	272.0817
2700K lighting	19.635	0.0985	0.0001	68.7121
Our method	18.5532	0.0617	-0.0035	84.1564

TABLE II: Average perceptual and biological metrics on screenshot images.

Method	ΔE	$\Delta u'v'$	D_{uv}	EML
Original (left-top)	0	0	-0.02	182.77
2700K lighting (right-top)	16.16	0.08	-0.02	47.66
Our method (right-down)	16.56	0.03	-0.01	81.56

TABLE III: Quantitative metrics for Case 1 (camera-captured indoor image).

5.51% in ΔE and 37.36% in $\Delta u'v'$ on screenshot images. In terms of biological impact, our method increases the EML by 39.17% on camera-captured images and 22.48% on screenshot images compared to the 2700K baseline. However, these values remain well below the original 6500K lighting, which only 36.46% and 30.93% of the original EML levels, respectively—suggesting a favorable trade-off between circadian safety and perceptual quality.

Although differences in image content, sensor characteristics, and compression artifacts may contribute to varying chromatic shifts between camera-captured and screenshot images under 2700K lighting, our results demonstrate that the proposed method consistently corrects these biases. In both cases, the compensated images exhibit D_{uv} values closely aligned with the original 6500K reference, indicating improved chromatic consistency and reduced perceptual distortion.

D. Qualitative Results

As illustrated in Fig. 5, the image captured under the 2700K lighting condition (top right) exhibits a noticeable red-orange cast, resulting in clear color distortion compared to the original image (top left). This is a common artifact in low-blue-light modes where blue attenuation is applied without proper compensation.

In contrast, the result produced by our proposed method (bottom right) appears more natural and visually closer to the original. While the ΔE remains comparable to that of the 2700K lighting (16.56 vs. 16.16), our method substantially improves chromatic consistency, reducing the $\Delta u'v'$ from 0.08 to 0.03. This indicates a significant perceptual improvement in color appearance.

Biologically, the EML increases from 47.66 to 81.56. However, it still represents only 44.62% of the original 6500K exposure level (182.77), suggesting that the method strikes a favorable balance between perceptual quality and circadian safety.

In another example, shown in Fig. 6, the image captured under the 2700K lighting condition causes the cat to become nearly indistinguishable from the background due to severe color distortion and reduced contrast. The object blends into the surroundings, making it difficult to recognize.



Fig. 5: Case 1 visual comparison

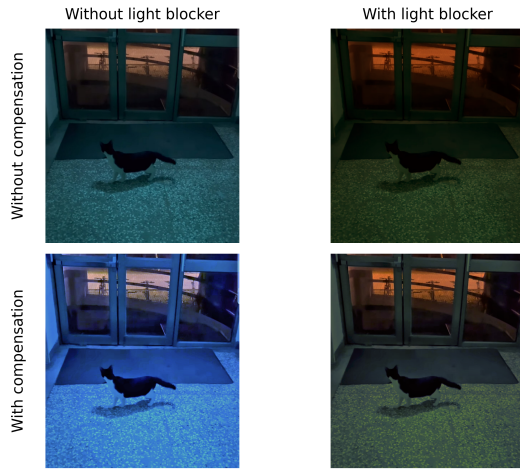


Fig. 6: Case 2 visual comparison

Our proposed method effectively resolves this issue, enhancing both color separation and visual clarity. As a result, the cat becomes clearly visible, and the overall image exhibits improved perceptual quality.

IV. CONCLUSION

In this work, we present a perceptual color compensation method tailored for low-blue-light display environments. Our

approach improves color fidelity under attenuated blue primaries while maintaining biologically safe melanopic light levels.

Quantitative results show that the proposed method significantly reduces perceptual color errors (by up to 46% in $\Delta u'v'$) while maintaining melanopic exposure at only 30–36% of the original 6500K baseline.

Overall, our method offers a compelling compromise between perceptual accuracy and circadian safety. By preserving visual quality while mitigating blue-light hazards, it eliminates the traditional trade-off between color realism and biological well-being.

REFERENCES

- [1] W. Xu et al., "Evaluation and application strategy of low blue light mode of desktop display based on brightness characteristics," *Displays*, vol. 84, p. 102809, Sep. 2024, doi: 10.1016/j.displa.2024.102809.
- [2] R. J. Lucas et al., "Measuring and using light in the melanopsin age," *Trends in Neurosciences*, vol. 37, no. 1, pp. 1–9, Jan. 2014, doi: 10.1016/j.tins.2013.10.004.
- [3] A. Nixon, R. Robillard, C. Leveille, et al., "Assessing the effects of polychromatic light exposure on mood in adults: A systematic review contrasting α -optic equivalent daylight illuminances," *LEUKOS*, vol. 20, no. 2, pp. 127–147, 2024.
- [4] J. Nilsson and T. Akenine-Möller, "Understanding SSIM," Jun. 29, 2020, arXiv: arXiv:2006.13846. doi: 10.48550/arXiv.2006.13846.
- [5] M. Afifi, B. Price, S. Cohen, and M. S. Brown, "When Color Constancy Goes Wrong: Correcting Improperly White-Balanced Images," in 2019 IEEE/CVF Conference on Computer Vision and Pattern Recognition (CVPR), Long Beach, CA, USA: IEEE, Jun. 2019, pp. 1535–1544. doi: 10.1109/CVPR.2019.00163.
- [6] G. Tan, J.-H. Lee, S.-C. Lin, R. Zhu, S.-H. Choi, and S.-T. Wu, "Analysis and optimization on the angular color shift of RGB OLED displays," *Opt. Express*, vol. 25, no. 26, p. 33629, Dec. 2017, doi: 10.1364/OE.25.033629.
- [7] F. Gou et al., "Angular color shift of micro-LED displays," *Opt. Express*, vol. 27, no. 12, p. A746, Jun. 2019, doi: 10.1364/OE.27.00A746.
- [8] K.-T. Shih and H. H. Chen, "Exploiting Perceptual Anchoring for Color Image Enhancement," *IEEE Trans. Multimedia*, vol. 18, no. 2, pp. 300–310, Feb. 2016, doi: 10.1109/TMM.2015.2503918.
- [9] K. A. G. Smet, "Two Neutral White Illumination Loci Based on Unique White Rating and Degree of Chromatic Adaptation," *LEUKOS*, vol. 14, no. 2, pp. 55–67, Apr. 2018, doi: 10.1080/15502724.2017.1385400.
- [10] K.-T. Shih, J.-S. Liu, F. Shyu, S.-L. Yeh, and H. H. Chen, "Blocking harmful blue light while preserving image color appearance," *ACM Trans. Graph.*, vol. 35, no. 6, pp. 1–10, Nov. 2016, doi: 10.1145/2980179.2982418.
- [11] OtoPhotonics, "SpectraSmart DS1200 User Manual." [Online]. Available: <https://www.otophotonics.com/pdf/285723/%E6%96%87%E4%BB%B6%E6%89%8B%E5%86%8A1.pdf>. Accessed: May 2025.
- [12] M. D. Fairchild, *Color Appearance Models*, 3rd ed. Chichester, U.K.: Wiley, 2013, doi: 10.1002/9781118653128

Method	ΔE	$\Delta u'v'$	Duv	EML
Original (left-top)	0	0	0.02	265.9
2700K lighting (right-top)	17.55	0.09	0.02	85.77
Our method (right-down)	17.77	0.04	0.01	102.36

TABLE IV: Quantitative metrics for Case 2 (screenshot cat image).